Argonne NATIONAL LABORATORY

ANL/RERTR/TM-12-28

# Conceptual Design Parameters for MITR LEU U-Mo Fuel Conversion Demonstration Experimental Irradiations

Nuclear Engineering Division

**About Argonne National Laboratory**

Argonne is a U.S. Department of Energy laboratory managed by UChicago Argonne, LLC under contract DE-AC02-06CH11357. The Laboratory's main facility is outside Chicago, at 9700 South Cass Avenue, Argonne, Illinois 60439. For information about Argonne and its pioneering science and technology programs, see www.anl.gov.

**Availability of This Report**

This report is available, at no cost, at http://www.osti.gov/bridge. It is also available on paper to the U.S. Department of Energy and its contractors, for a processing fee, from:

U.S. Department of Energy
Office of Scientific and Technical Information
P.O. Box 62
Oak Ridge, TN 37831-0062
phone (865) 576-8401
fax (865) 576-5728
reports@adonis.osti.gov

ANL/RERTR/TM-12-28

# Conceptual Design Parameters for MITR LEU U-Mo Fuel Conversion Demonstration Experimental Irradiations

by
Erik H. Wilson[1], Thomas H. Newton, Jr.[2], Lin-wen Hu[2], Floyd E. Dunn[1], and John G. Stevens[1]
[1]Nuclear Engineering Division, Argonne National Laboratory
[2]MIT Nuclear Reactor Laboratory and Nuclear Science and Engineering Department

June 21, 2012

This work is sponsored by the U.S. Department of Energy,
National Nuclear Security Administration Office of Global Threat Reduction (NA-21)

# Abstract

The Massachusetts Institute of Technology Reactor (MITR-II) is a research reactor in Cambridge, Massachusetts designed primarily for experiments using neutron beam and in-core irradiation facilities. It delivers a neutron flux comparable to current LWR power reactors in a compact 6 MW core using Highly Enriched Uranium (HEU) fuel.

In the framework of its non-proliferation policies, the international community presently aims to minimize the amount of nuclear material available that could be used for nuclear weapons. In this geopolitical context, most research and test reactors both domestic and international have started a program of conversion to the use of Low Enriched Uranium (LEU) fuel. A new type of LEU fuel based on an alloy of uranium and molybdenum (UMo) is expected to allow the conversion of U.S. domestic high performance reactors like the MITR-II reactor. Toward specifying requirements for Design Demonstration Experiment (DDE) Irradiations in a test reactor, a key set of conceptual design parameters are presented for MITR LEU monolithic U-Mo alloy fuel with 10 wt% Mo.

# Table of Contents

# Table of Figures

# List of Tables

# 1 Introduction

The Massachusetts Institute of Technology Reactor (MITR-II) is a research reactor in Cambridge, Massachusetts designed primarily for experiments using neutron beam and in-core irradiation facilities. It delivers a neutron flux comparable to current LWR power reactors in a compact 6 MW core using Highly Enriched Uranium (HEU) fuel.

In the framework of its non-proliferation policies, the international community presently aims to minimize the amount of nuclear material available that could potentially be diverted for nuclear weapons. In this geopolitical context, most research and test reactors both domestic and international have started a program of conversion to the use of Low Enriched Uranium (LEU) fuel. A new type of LEU fuel based on an alloy of uranium and molybdenum (UMo) is expected to allow the conversion of compact high performance reactors like the MITR-II reactor.

Safety analyses of an MITR core fueled with a monolithic alloy of uranium and 10 wt% molybdenum (U-10Mo) have been conducted to establish the steady state safety basis of the reactor using the feasibility design of the MITR reactor [1] [2] [3]. The thermal hydraulic analyses of the reactor have required detailed power distributions and geometrical considerations in order to identify regions of interest for safety analyses [4]. The feasibility design referenced in [5] has been used throughout the works previously referenced. This set of analyses, performed with the feasibility design, serve as the reference for key parameters to be used in the conceptual design of the irradiation of the Design Demonstration Experiment (DDE) in a test reactor prior to conversion of MITR with the same LEU plate geometry and fabrication.

# 2 Geometry of LEU Core

The MIT Reactor (MITR-II) core has a hexagonal design that contains twenty-seven fuel positions in three radial rings (A, B, and C), as shown in Figure 1. Typically three of these positions (two in the A-ring and one in the B-ring) are filled with either an in-core experimental facility or a solid aluminum dummy element to reduce power peaking. The remaining positions are filled with standard MITR-II fuel elements.

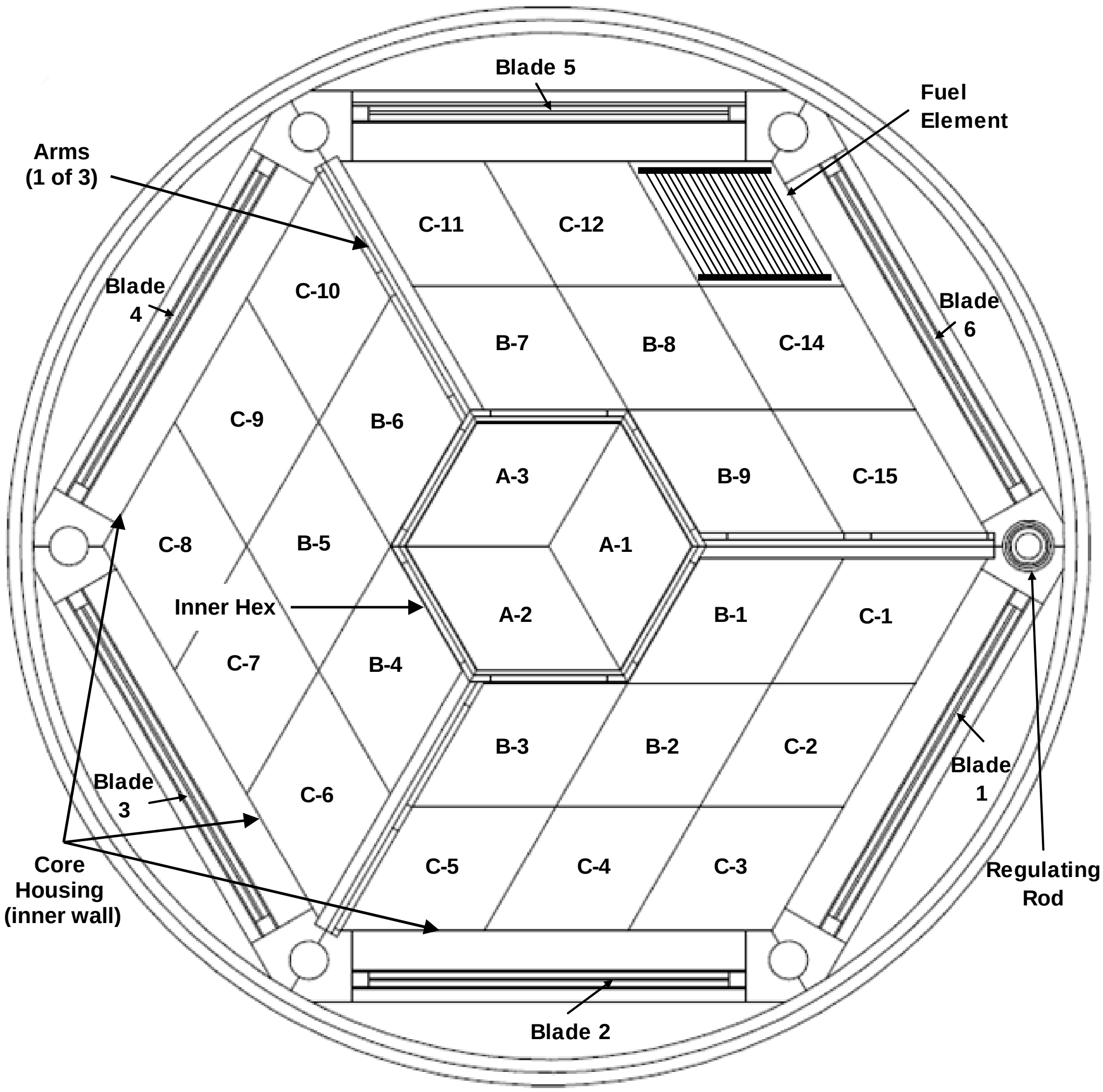


Figure 1. Layout of the MIT reactor core.

## 2.1 Nominal Element Geometry

The feasibility LEU design was discussed in [5]. Each rhomboid-shaped LEU fuel element contains eighteen aluminum-clad fuel plates with a fuel zone thickness of 0.508 mm (0.020 inch) and fuel zone length of 56.8325 cm (22.375 inch). The LEU fuel modeled is a uranium-molybdenum monolithic alloy enriched up to 19.75% $^{235}U$, and with 10 wt% Mo at an overall fuel density of 17.02 g/cm$^3$. The cladding, (consisting of 6061 aluminum alloy and a thin zirconium layer at the fuel interface) of each fuel plate is 0.254 mm (0.010 inch) thick. In order to increase heat transfer to the coolant, there are 0.254 mm (0.010 inch) longitudinal fins in addition to the 0.254 mm (0.010 inch) cladding (Zr interlayer and 6061 aluminum). The thickness of the fuel plate is 1.524 mm (0.060 inch) from fin-tip to fin-tip.

The gaps between fuel plates which form the coolant channels within an element are referred to as interior channels. These interior channels are 0.072 inch from fin-tip to fin-tip. End channels are present on the outside of the outer fuel plates. Table 1 lists dimensions of the LEU element, as illustrated schematically (not to scale) in Figures 2-3. The LEU element design, other than as noted, is based upon the MITR HEU fuel element drawing specification shown in Figure 4 [6]. Figures 5 and 6 illustrate fuel element end channels with a neighboring element and also with structural walls. Note that the dimension mil represents 0.001 inches or 0.0254 millimeters.

Table 1. HEU and LEU element dimensions.

| | **Plate and Channel Dimensions (Schematic Labels Figs. 2-3)** | **HEU** | **LEU** |
|---|---|---|---|
| | Fuel plate length (inch) | 23 | 23 |
| | Fuel meat length (inch) | 22.375 | 22.375 |
| | Fuel plates per assembly | 15 | 18 |
| | Interior (full) channels per assembly | 14 | 17 |
| | End (partial) channels per assembly | 2 | 2 |
| (a) | Fuel meat thickness (mil) | 30 | 20 |
| (b) | Fuel meat width (inch)[a] | 2.082 | 2.082 |
| (c) | Clad thickness (base of fin to fuel surface) | 15 (6061 Al) | 10 (6061Al + Zr) |
| (d) | Plate to plate pitch, CL to CL (mil) | 158 | 132 |
| (e) | Interior channel water gap (fin tip-to-tip) (mil) | 78 | 72 |
| (f) | Effective interior channel thickness (mil) | 88 | 82 |
| (g) | Finned width (inch)[a] | 2.2 | 2.2 |
| | Number of fins per plate | 110 per side | 110 per side |
| (h) | Fin depth (mil) | 10 | 10 |
| (i) | Fin width (mil) | 10 | 10 |
| (j) | Width between fuel meat and side plate (mil) | 113 | 113 |
| (k) | Width between fins and side plate (mil) | 54 | 54 |
| (l) | Channel width (inch)[a] | 2.308 | 2.308 |
| (m) | Side plate thickness (mil) | 188 | 188 |
| (n) | Side plate flat-to-flat, outer edge of one side plate to outer edge of second side plate on element (inch) | 2.375 | 2.375 |
| (o) | Element end flat-to-flat (inch) | 2.380 | 2.380 |
| (p) | Outer plate fin-tip to side plate end plane (mil) | 44 | 38 |
| (q) | Effective outer plate gap to side plate end plane (mil) | 49 | 43 |
| | Outer plate fin-tip to nozzle at full width (mil)[b] | 56.5 | 50.5 |
| | Effective outer plate gap to nozzle at full width (mil) | 61.5 | 55.5 |

[a] For thermal hydraulic analysis, channel width is the fuel meat width of 2.082 inch (0.052883 m) due to treatment in section 4.1 accounting for conductive cooling using the 2.308 channel width.

[b] As illustrated in Figure 5, dimension (b). This dimension represents the limiting case of an assembly nozzle touching the adjacent structural wall as discussed in [4].

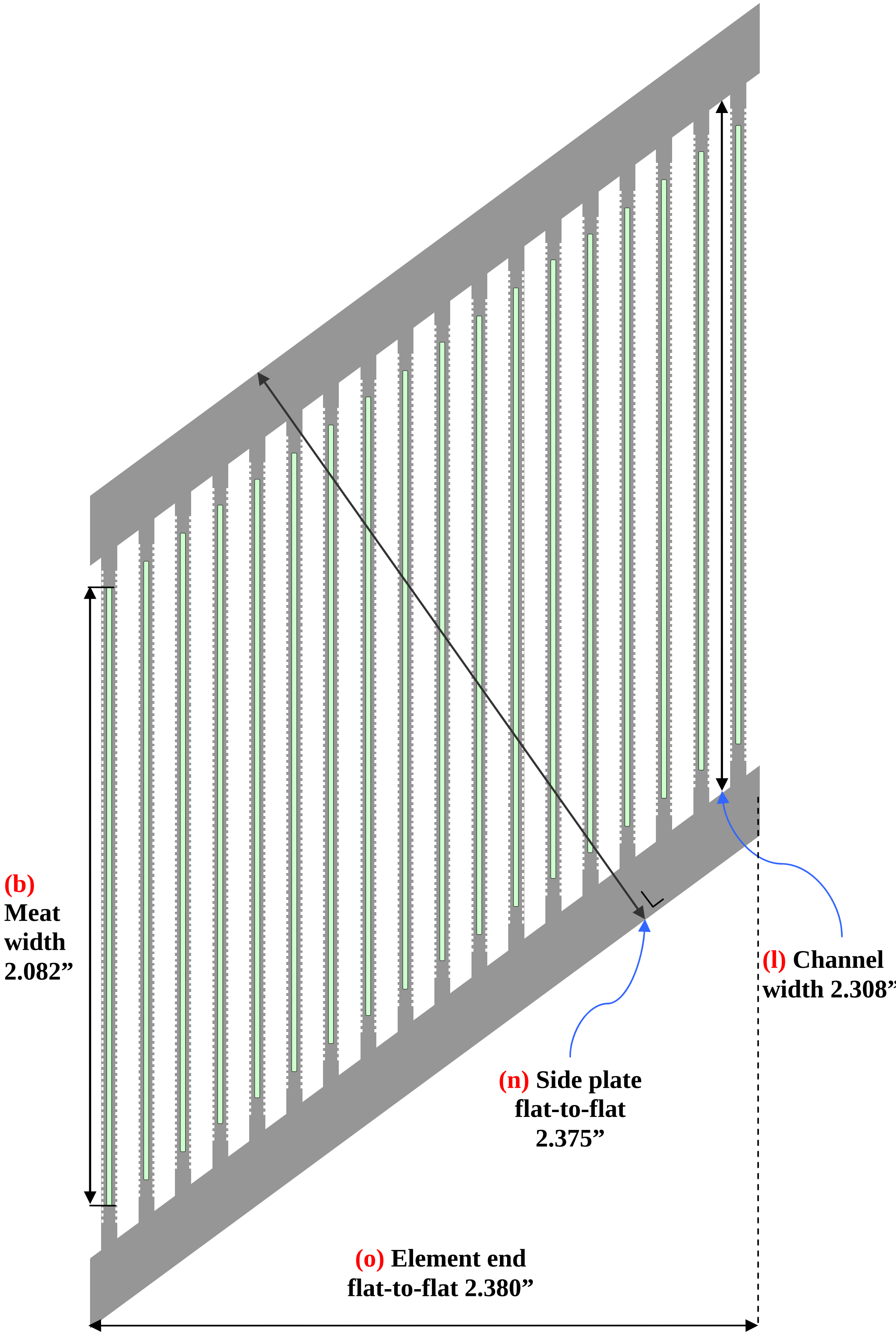


Figure 2. Schematic of MITR LEU fuel element drawn with 18 plates.
(letters indicate dimensions listed in Table 1)

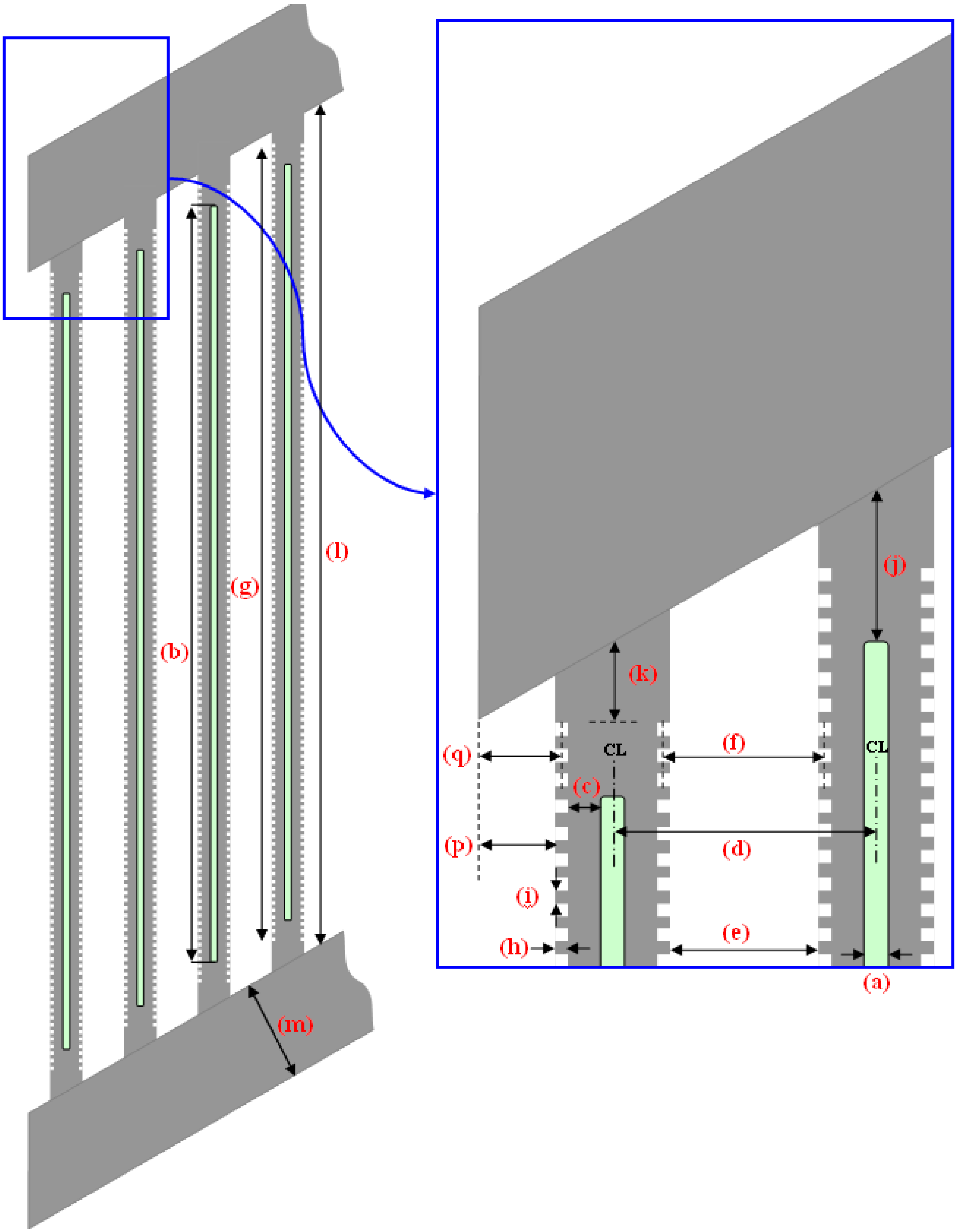


Figure 3. Schematic of MITR LEU fuel element (outer 4 of 18 plates shown).
(letters indicate dimensions listed in Table 1)

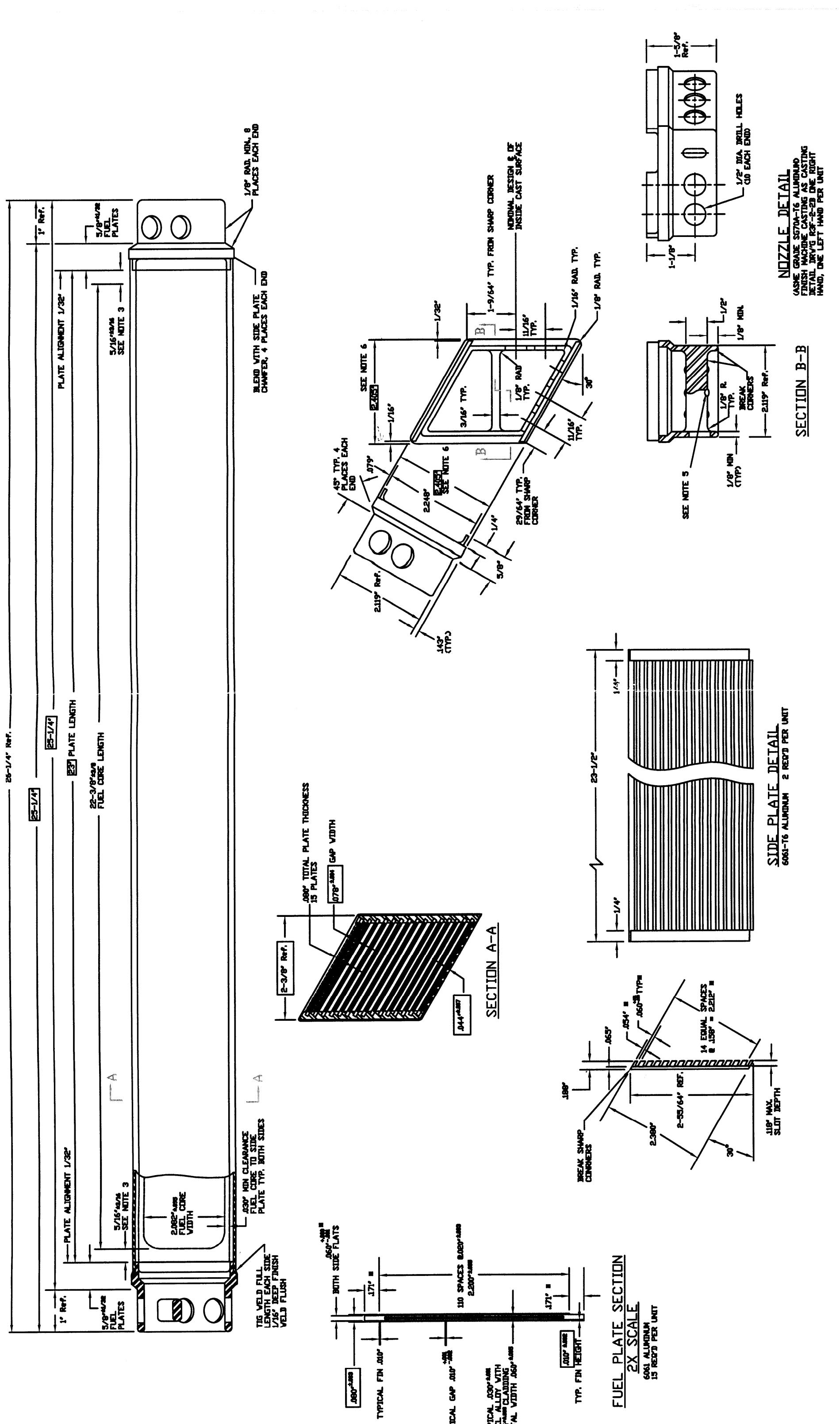


Figure 4. HEU fuel element MITR specification R3F-201-4.

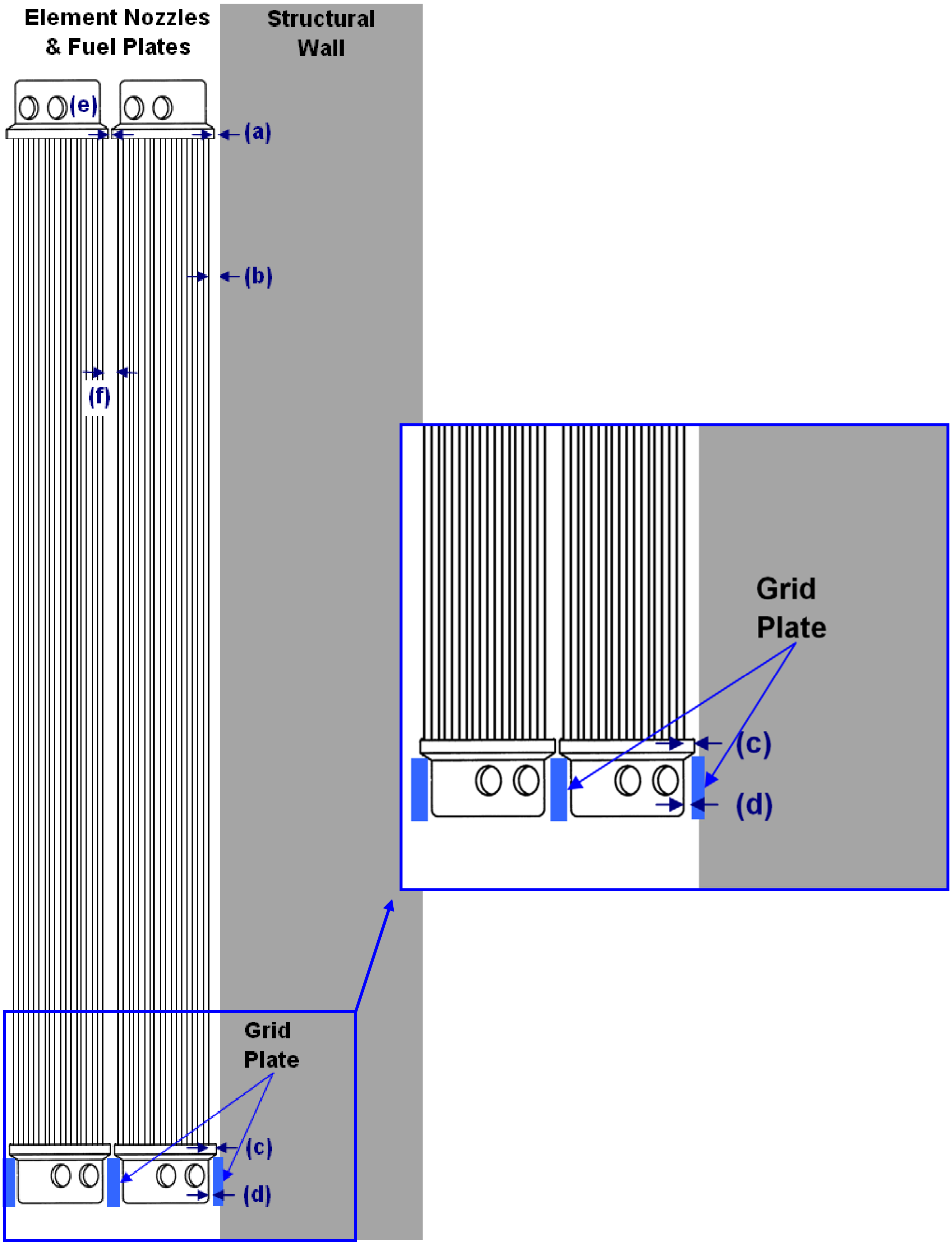


Figure 5. Cross-section of fuel elements illustrating end channels (side plates not shown).
(letters indicate dimensions listed in Table 2)

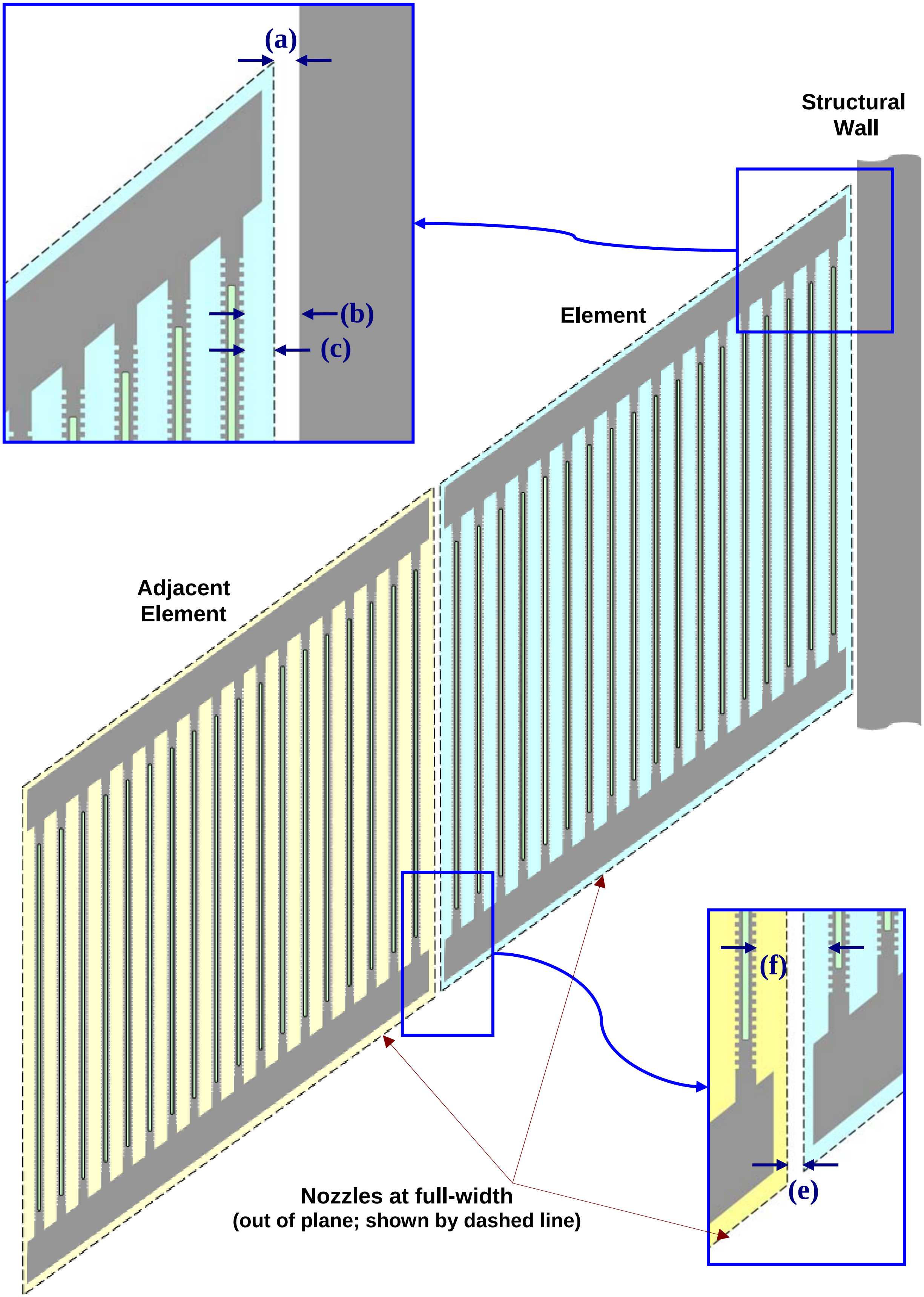


Figure 6. Cross-section of LEU element with neighboring element and structural wall, top view. (letters indicate dimensions listed in Table 2)

Table 2 gives the various nominal dimensions of an end channel for the limiting case, a C-ring end channel facing the core housing. For purposes of the DDE irradiation, the appropriate end channel dimension is 50.5 mil from the fin tip to the wall opposite the element. This corresponds to a nominally-built element with the end nozzles touching a structural wall. End nozzles touching a wall is representative since the element has some freedom of movement when loaded into the reactor sufficient to allow contact. This case is illustrated in Figures 5 and 6 where the dimension (a) is assumed, due to freedom of movement, to be zero with end nozzle to wall contact.

Table 2. Nominal dimensions in end channels of LEU elements facing core housing (C-ring).

| **Schematic Label (Figs. 5-6)** | **Gap between Components** | **Dimension (mil)** |
|---|---|---|
| (a) | Nozzle to core housing wall | 15 [a] |
| (b) | Fin-tip to core housing wall | 65.5 [a] |
| (c) | Fuel plate fin-tip to full-width of nozzle | 50.5 |
| (d) | Nozzle insert to grid plate | 13 |
| (e) | Gap between nozzles | 10 [a] |
| (f) | End channel between adjacent elements (fuel plate fin-tip to fin-tip) | 111 [a] |

[a] Listed for limiting case of C-ring element end channel facing the core housing as discussed in [4].

# 3 Limiting LEU Power Distribution

In order to characterize power distributions over a range of MITR LEU core configurations, a set of depleted cores was generated [4]. The most limiting case, in terms of both power and thermal hydraulics was found for a depleted MITR LEU Core 189, and is described below [3].

## 3.1 Calculation Methodology for Power Distributions

Power distributions for the power profiles reported are based upon an MCODE [7] depletion using ORIGEN2 [8] with independently depleting spatial zones in MCNP5 [9] as given in Table 3. All calculations of heat flux are based upon an area of fuel meat (referred to as foil for LEU) without considering any additional area for the fins or un-fueled regions on either side of the foil. Thus, the area used to calculate heat flux from the fueled portion of each plate is both sides of the fuel meat zone 22.375 inches in length and 2.082 inches in width. Consideration of the additional heat transfer provided by fins is not taken into account during calculation of power distributions, but instead in the thermal hydraulic modeling of MITR.

Table 3. Discretization of the LEU depletion zones and power regions used to generate neutronic power shapes in the peak plates.

| Spatial Regions | MCNP Model Geometry | Depletion | Power Shape |
|---|---|---|---|
| Fuel foil axial region (cm of foil) | Continuous | 9.47 | 3.16 |
| Fuel foil lateral region (cm of foil) | Continuous | 5.29 | 1.32 |

Power distributions are generated by dividing each plate into four equal stripes along the 2.082 inch width. The four stripes were shown in [4] to represent the power peaking at the outside of each plate without explicitly taking into account lateral heat conduction. Since the lateral division is based upon this analysis, the results presented in this work are intended only for use in a thermal hydraulic analysis which does not explicitly model or otherwise incorporate the effects of lateral heat conduction.

A comparative basis should be maintained between the calculations referenced in this work that will form the LEU safety basis, and the DDE irradiations. To this end, unless there is a specific rationale, the size scale of regions of depletion and power distribution used for DDE irradiation planning and results should correspond with those used in this work in order to represent the various physical phenomena accounted for in the safety basis calculations. Where variations exist the DDE irradiation planning should compare results based on the discretization presented in this work in order to ensure that alterations do not impact accurate modeling of the underlying phenomena.

With the discretization used for generation of the power distributions, each axial region is 3.16 cm tall, and each stripe 1.32 cm wide laterally along the whole axial length of each plate. Thus with 18 axial regions, the smallest region is the intersection of these comprising a region of 4.17 $cm^2$ of fuel meat area which is referred to as a “location” or “spot”.

## 3.2 Limiting Power Distributions of LEU Cores

The most limiting power profile for is the maximum power stripe of Core 189 End of Cycle (EOC), where Figure 7 and Table 4 give the axial heat flux profile of this stripe for a 7 MW core power. The same plate contains the single location (spot) of maximum heat flux at the beginning of cycle- Core 189 Beginning of Cycle (BOC). The power distribution for the entire plate containing these peak locations is shown in Figures 8 and 9, and is listed in Table 5a for a 7 MW core power. In these power profiles the peak stripe power is 57.2 W/cm$^2$ of foil (axially-averaged), and the peak single location is a spot with 76.6 W/cm$^2$ of foil. Various extrema and peaking factors for Core 189 are listed in Table 5b for the same peak plate listed in Table 5a. The peaking factor "stripe peaking within plate" is defined as the average heat flux of a stripe (a fuel foil is divided into four equal stripes along the 2.082 inch width) divided by the average heat flux of the plate in which the stripe resides. The peaking factor "local peaking within stripe" is defined as the local heat flux of a spot divided by the average heat flux of the stripe in which the spot resides (a spot is one segment of a stripe after division into 18 axial segments).

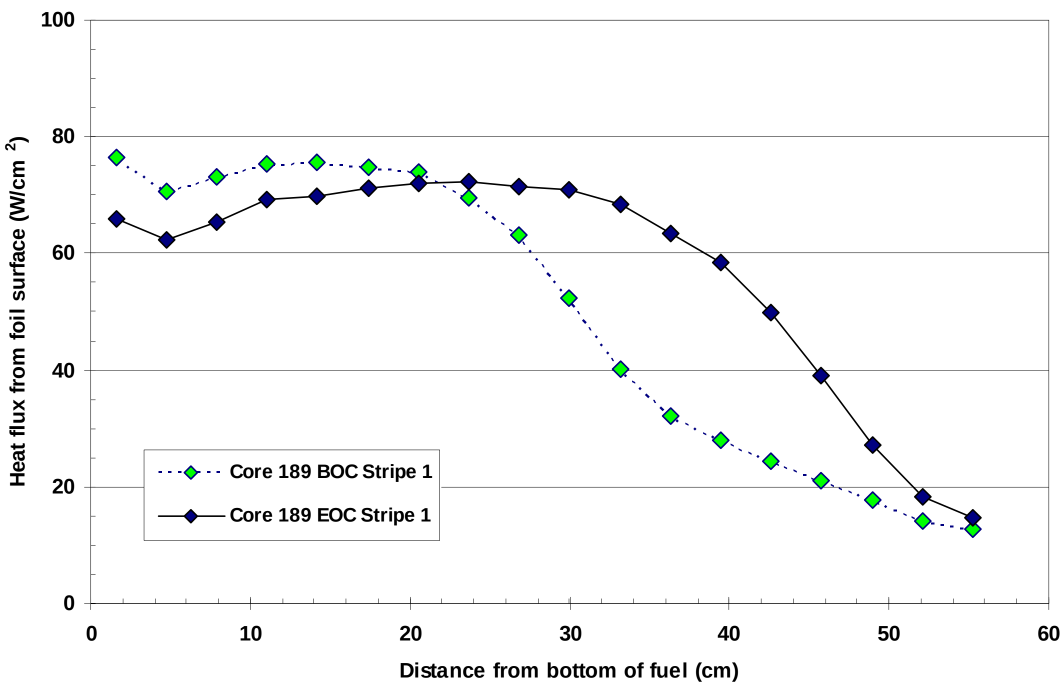


Figure 7. Axial heat flux profile of location (Core 189 BOC) and stripe (Core 189 EOC) of maximum heat flux.

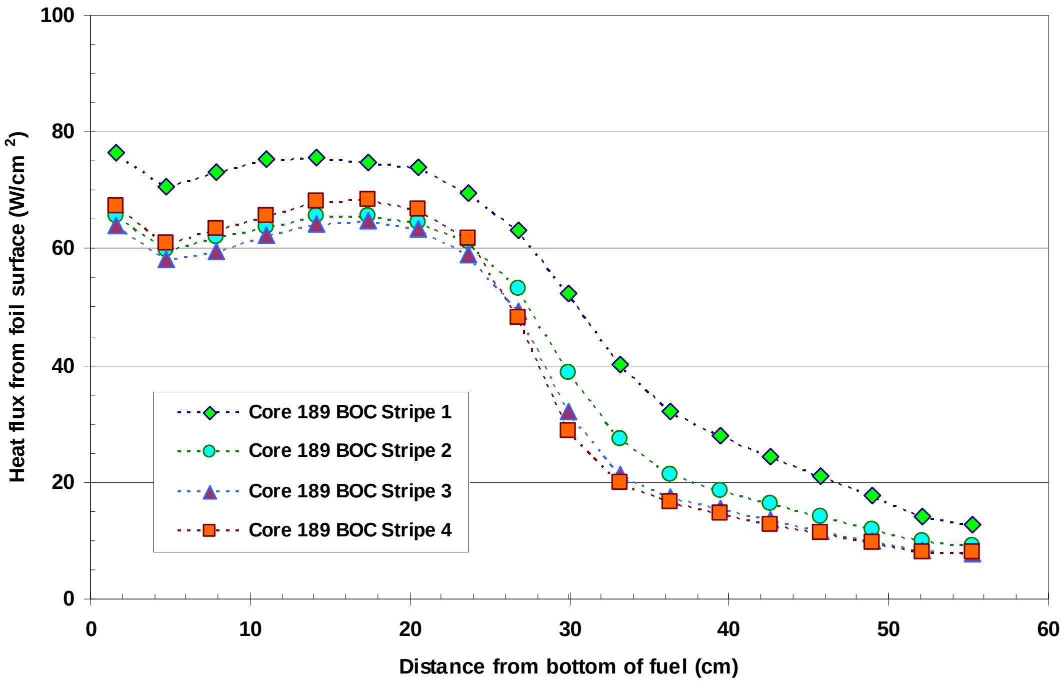


Figure 8. Axial heat flux profile of LEU plate with location of maximum heat flux.

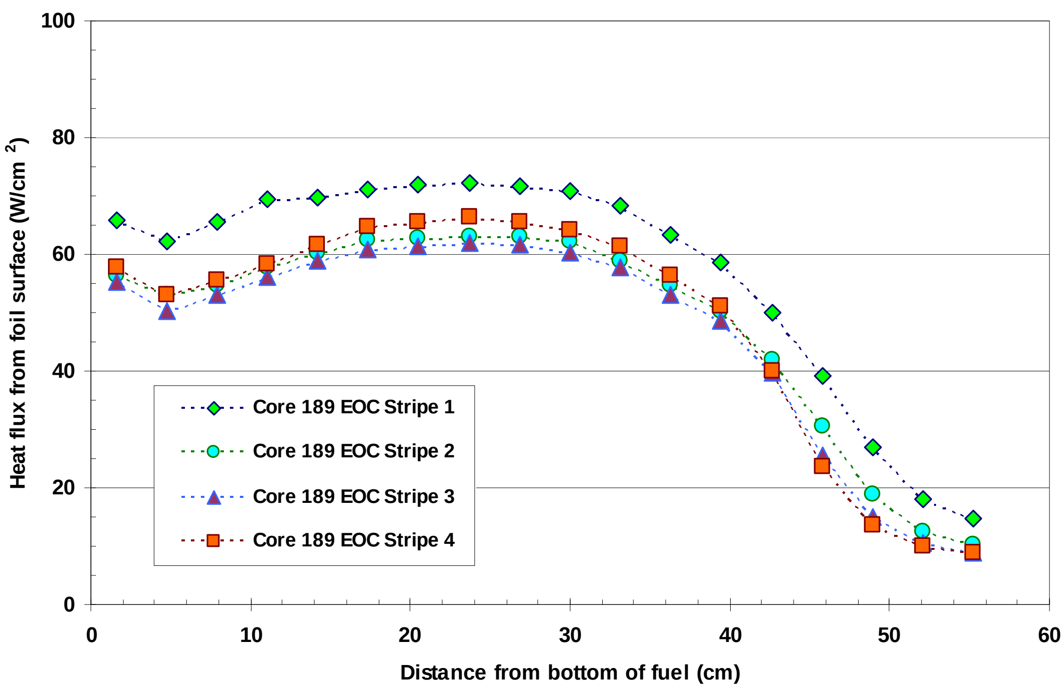


Figure 9. Axial heat flux profile of LEU plate with stripe of maximum heat flux.

Table 4. Axial heat flux distributions of 7 MW LEU cores with locations of maximum power.

| | Heat Flux (W/cm$^2$ of foil) | |
|---|---|---|
| **Distance of Axial Node Center from Bottom of Fuel (cm)** | **Stripe with Peak Spot (Core 189 BOC Stripe 1)** | **Peak Stripe (Core 189 EOC Stripe 1)** |
| 55.3 | 12.8 | 14.6 |
| 52.1 | 14.2 | 18.2 |
| 48.9 | 17.7 | 27.1 |
| 45.8 | 21.0 | 39.1 |
| 42.6 | 24.4 | 50.0 |
| 39.5 | 28.0 | 58.6 |
| 36.3 | 32.1 | 63.3 |
| 33.2 | 40.2 | 68.5 |
| 30.0 | 52.4 | 70.9 |
| 26.8 | 63.1 | 71.6 |
| 23.7 | 69.6 | 72.2 |
| 20.5 | 73.9 | 71.9 |
| 17.4 | 74.8 | 71.1 |
| 14.2 | 75.7 | 69.7 |
| 11.1 | 75.3 | 69.3 |
| 7.9 | 73.0 | 65.5 |
| 4.7 | 70.6 | 62.3 |
| 1.6 | 76.6 | 66.0 |
| **Stripe Average (W/cm$^2$ of foil)** | 49.7 | 57.2 |

[a] Top of LEU fuel foil in upflow reactor is at 22 ⅜ inch (56.8325 cm).
[b] Bottom of LEU fuel foil upflow reactor is at zero.

Table 5a. Axial heat flux distributions of 7 MW LEU cores in plate with locations of maximum power.

| | Heat Flux (W/cm$^2$ of foil) | | | | | | | |
|---|---|---|---|---|---|---|---|---|
| **Distance of Axial Node Center from Bottom of Fuel (cm)** | **Core 189 BOC Stripe 1** | **Core 189 BOC Stripe 2** | **Core 189 BOC Stripe 3** | **Core 189 BOC Stripe 4** | **Core 189 EOC Stripe 1** | **Core 189 EOC Stripe 2** | **Core 189 EOC Stripe 3** | **Core 189 EOC Stripe 4** |
| 55.3 [a] | 12.8 | 9.2 | 7.9 | 8.1 | 14.6 | 10.4 | 8.9 | 8.9 |
| 52.1 | 14.2 | 9.9 | 8.3 | 8.1 | 18.2 | 12.4 | 10.4 | 9.9 |
| 48.9 | 17.7 | 12.0 | 9.9 | 9.6 | 27.1 | 19.0 | 15.0 | 13.7 |
| 45.8 | 21.0 | 14.1 | 11.7 | 11.2 | 39.1 | 30.5 | 25.5 | 23.7 |
| 42.6 | 24.4 | 16.4 | 13.5 | 12.8 | 50.0 | 42.0 | 39.7 | 40.0 |
| 39.5 | 28.0 | 18.5 | 15.4 | 14.6 | 58.6 | 50.3 | 48.7 | 51.2 |
| 36.3 | 32.1 | 21.4 | 17.4 | 16.5 | 63.3 | 54.6 | 53.0 | 56.4 |
| 33.2 | 40.2 | 27.3 | 21.3 | 19.9 | 68.5 | 58.8 | 57.9 | 61.3 |
| 30.0 | 52.4 | 38.9 | 32.1 | 28.8 | 70.9 | 62.1 | 60.3 | 64.1 |
| 26.8 | 63.1 | 53.0 | 49.3 | 48.2 | 71.6 | 63.0 | 61.8 | 65.5 |
| 23.7 | 69.6 | 61.1 | 59.1 | 61.8 | 72.2 | 62.9 | 62.0 | 66.3 |
| 20.5 | 73.9 | 64.6 | 63.4 | 66.8 | 71.9 | 62.7 | 61.5 | 65.6 |
| 17.4 | 74.8 | 65.7 | 64.8 | 68.6 | 71.1 | 62.4 | 61.0 | 64.6 |
| 14.2 | 75.7 | 65.7 | 64.3 | 68.2 | 69.7 | 60.2 | 58.8 | 61.6 |
| 11.1 | 75.3 | 63.8 | 62.2 | 65.7 | 69.3 | 57.8 | 56.2 | 58.4 |
| 7.9 | 73.0 | 62.1 | 59.6 | 63.5 | 65.5 | 54.8 | 53.1 | 55.7 |
| 4.7 | 70.6 | 59.9 | 58.2 | 60.9 | 62.3 | 53.0 | 50.4 | 53.0 |
| 1.6 [b] | 76.6 | 65.7 | 64.1 | 67.4 | 66.0 | 56.5 | 55.2 | 57.8 |
| **Stripe Average** | 49.7 | 40.5 | 37.9 | 38.9 | 57.2 | 48.5 | 46.6 | 48.8 |

[a] Top of LEU fuel foil in upflow reactor is at 22 ⅜ inch (56.8325 cm).
[b] Bottom of LEU fuel foil in upflow reactor is at zero.

Table 5b. Extrema and peaking in plate of 7 MW LEU cores with locations of maximum power.

| | **Core 189 BOC Stripe 1** | **Core 189 BOC Stripe 2** | **Core 189 BOC Stripe 3** | **Core 189 BOC Stripe 4** | **Core 189 EOC Stripe 1** | **Core 189 EOC Stripe 2** | **Core 189 EOC Stripe 3** | **Core 189 EOC Stripe 4** |
|---|---|---|---|---|---|---|---|---|
| Local Peaking within Stripe | 1.54 | 1.62 | 1.71 | 1.76 | 2.26 | 1.30 | 1.33 | 1.36 |
| Stripe Peaking within Plate | 1.19 | 0.97 | 0.91 | 0.93 | 1.14 | 0.97 | 0.93 | 0.97 |
| Average Power in Plate | 41.8 W/cm$^2$ of foil | | | | 50.3 W/cm$^2$ of foil | | | |
| Peak Stripe Power in Plate | 49.7 W/cm$^2$ of foil | | | | 57.2 W/cm$^2$ of foil | | | |
| Peak Power in Plate | 76.6 W/cm$^2$ of foil | | | | 72.2 W/cm$^2$ of foil | | | |
| Minimum Stripe Power in Plate | 37.9 W/cm$^2$ of foil | | | | 46.6 W/cm$^2$ of foil | | | |
| Minimum Power in Plate | 7.9 W/cm$^2$ of foil | | | | 8.9 W/cm$^2$ of foil | | | |

Table 6 gives the burnup state of the peak spot and peak stripe among the depleted cores which occurred for Core 189 BOC and EOC, respectively. While these values represent burnup at the time of peak power, this burnup does not reflect the maximum levels of burnup anticipated for MITR LEU fuel, which are anticipated to be in excess of 50% $^{235}U$ burnup at peak locations.

In order to calculate $^{235}U$ fission density, the reference as-fabricated nominal density for $^{235}U$ is assumed to be $7.75 \times 10^{21}$ atoms/cm$^3$ [1]. DDE irradiation planning and results should state whether burnup is referenced in terms of $^{235}U$, as is the case in this report and reference [10] which stated, "in the RERTR program burn-up is defined as $^{235}U$ depletion from $^{235}U$ fissions alone."

Table 6. Axial burnup distribution of LEU cores with maximum heat flux locations.

| Axial Segment | Distance of Axial Node Center from Bottom of Fuel | Core 189 BOC Peak stripe | Core 189 EOC Peak stripe |
|---|---|---|---|
| | (cm) | $^{235}U$ Burnup % | $^{235}U$ Burnup % |
| 1 | 55.3 | 6.2 | 7.2 |
| 2 | 52.1 | 6.2 | 7.2 |
| 3 | 48.9 | 6.2 | 7.2 |
| 4 | 45.8 | 8.3 | 10.9 |
| 5 | 42.6 | 8.3 | 10.9 |
| 6 | 39.5 | 8.3 | 10.9 |
| 7 | 36.3 | 10.2 | 14.5 |
| 8 | 33.2 | 10.2 | 14.5 |
| 9 | 30.0 | 10.2 | 14.5 |
| 10 | 26.8 | 10.6 | 15.6 |
| 11 | 23.7 | 10.6 | 15.6 |
| 12 | 20.5 | 10.6 | 15.6 |
| 13 | 17.4 | 9.7 | 14.4 |
| 14 | 14.2 | 9.7 | 14.4 |
| 15 | 11.1 | 9.7 | 14.4 |
| 16 | 7.9 | 8.5 | 12.9 |
| 17 | 4.7 | 8.5 | 12.9 |
| 18 | 1.6 | 8.5 | 12.9 |

### 3.3 Power Ramping during Fuel Lifetime

Since the limiting power distributions occur in well-depleted elements, the fission rate in MITR elements with limiting power distributions will increase after the initial irradiation cycles. This phenomena occurs when elements are moved from the inner rings of core loading to the outer ring since power peaking is much higher for the fuel immediately adjacent to the heavy water reflector. An increase of power peaking in depleted fuel is known to be a consideration for fuel failures, and limits have previously been quantified for existing fuel systems, such as aluminide fuels, in order to avoid fuel performance issues.

The MITR DDE irradiations should reproduce the phenomena of power ramping over the life of the fuel for this reason. Any prior work in the fuel qualification of U-10Mo fuel where power was increased later in the life of the fuel should be listed in order to corroborate that fuel performance is acceptable for power increases later in the life of the depleted MITR DDE U-10Mo elements.

Figure 10 shows the increase in power peaking later in the life of an MITR element. The figure plots the axial power distribution of the heat flux (q") for a 7 MW core from the foil stripe of the element which is the most thermal hydraulically limiting of all MITR cores analyzed. This most limiting power distribution occurs for stripe 1 of element 27 plate 1 in Core 189 EOC. The remainder of the cores in which this plate is loaded are shown at BOC and EOC in Figure 10 as the third axis. This element, MIT-335, is loaded for Cores 179-181 and 189-190, and has an approximately similar power during the cores where it resides in the interior of the core (B-ring during Cores 179-181). In the core interior, flux shape is flatter and hence a more uniform heat flux is generated in the plates of each element. After a period of storage, the element was loaded for Cores 189-190 into a C-ring location, at which point the peak power occurred for the plate adjacent to the reflector with the heat flux profile and burnup as listed in Tables 5-6.

The magnitude of the heat flux was highest of any depleted MITR core for this element at Core 189 BOC for the single location where power peaked in a spot with 76.6 W/cm$^2$ of foil. At least as important for DDE irradiations is the magnitude and shape of the peak stripe of all MITR cores analyzed (peak stripe 57.2 W/cm2 of foil) at Core 189 EOC. The shapes of these peak distributions are shown in Figure 7, and the 2-D power profile of the plate is shown in Figure 8.

Whereas the plate distributions shown in Figure 8 remain important in order to represent the spatial rate of power change characteristic of MITR, Figure 10 illustrates increase in power over time. Stripe power increased by 63% and spot power by 43% when moved to the outer fuel ring, as listed in Table 7 despite being significantly depleted (see Table 6). Table 8 presents Core 179 2-D plate power profiles for the plate which peaks during Core 189.

Table 7. Power characteristic of plate with highest power at both initial loading into interior fuel rings, and later in life at time of highest power (when loaded into outer fuel ring).

| **Peak Power Region (element MIT-335)** | **Peak Power vs. Fuel Loading Position** | | **Increase in Power During Fuel Life (peak outer/inner)** |
|---|---|---|---|
| | **Inner Fuel Ring** | **Outer Fuel Ring** | |
| Peak Location Power (W/cm$^2$, single spot of foil) | 46.9 (Core 179 BOC) | 76.6 (Core 189 BOC) | 43% |
| Peak Stripe Power (W/cm$^2$ of foil, axially averaged) | 39.9 (Core 179 BOC) | 57.2 (Core 189 EOC) | 63% |

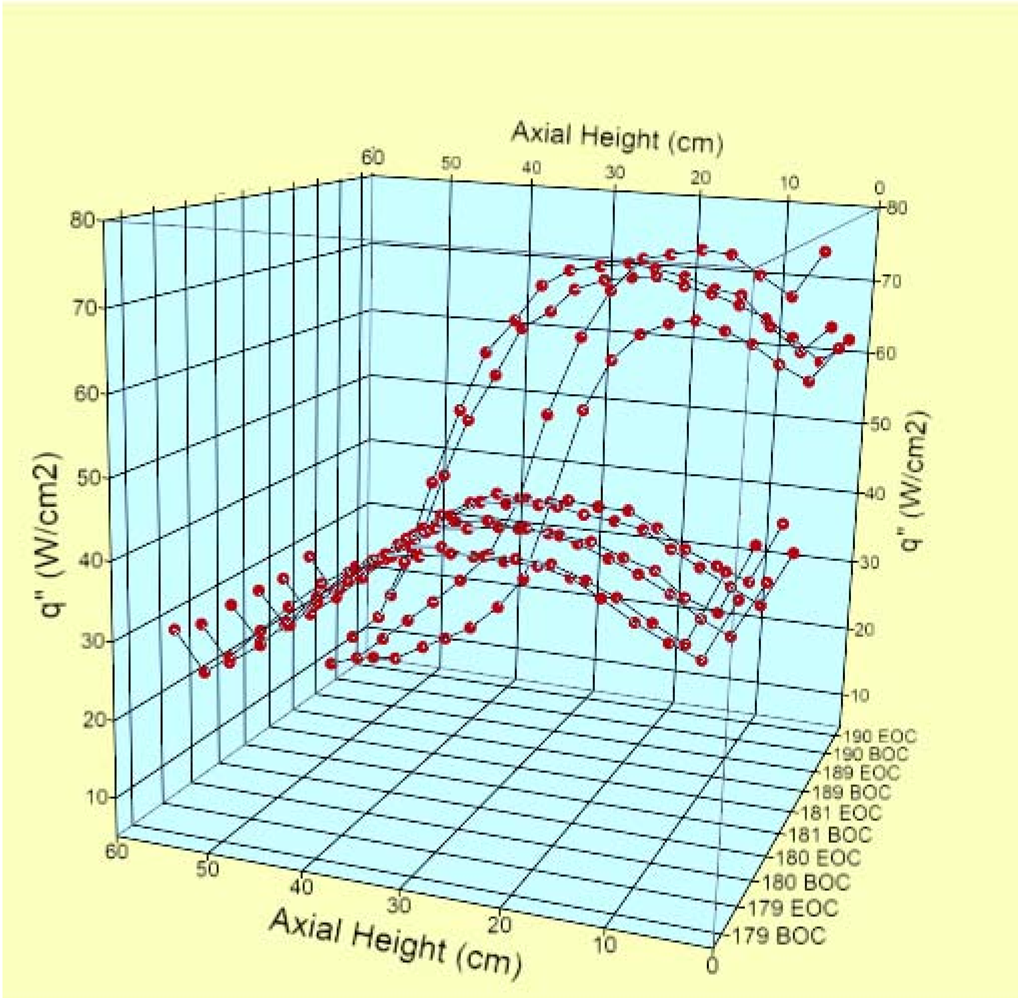


Figure 10. Axial heat flux (q") distribution for element of highest power (MIT-335) during the fuel shuffling sequence of Cores 179-190. Peak heat flux occurs during Core 189 EOC in a well-depleted element due to movement adjacent to $D_2O$ reflector. Earlier cycles show that the nearly fresh element power is >50% lower. Each curve shows q" vs. axial height from bottom of the fuel in the upflow MITR reactor.

Table 8. Axial power distribution of element MIT-335 plate 1 when loaded into interior fuel ring position B1 during LEU Core 179.

| | Heat Flux (W/cm$^2$ of foil) | | | | | | | |
|---|---|---|---|---|---|---|---|---|
| **Distance of Axial Node Center from Bottom of Fuel (cm)** | **Core 179 BOC Stripe 1** | **Core 179 BOC Stripe 2** | **Core 179 BOC Stripe 3** | **Core 179 BOC Stripe 4** | **Core 179 EOC Stripe 1** | **Core 179 EOC Stripe 2** | **Core 179 EOC Stripe 3** | **Core 179 EOC Stripe 4** |
| 55.3 [a] | 31.1 | 21.8 | 20.0 | 21.6 | 29.8 | 21.4 | 19.6 | 21.1 |
| 52.1 | 26.2 | 18.8 | 17.0 | 17.8 | 25.5 | 18.2 | 16.6 | 17.7 |
| 48.9 | 29.0 | 21.8 | 20.1 | 20.8 | 28.2 | 21.3 | 19.7 | 20.8 |
| 45.8 | 32.8 | 24.9 | 22.8 | 24.1 | 31.8 | 24.5 | 22.8 | 23.8 |
| 42.6 | 36.5 | 28.0 | 25.8 | 26.9 | 35.5 | 27.6 | 25.5 | 27.1 |
| 39.5 | 39.6 | 30.6 | 28.8 | 29.9 | 38.9 | 30.0 | 28.0 | 30.3 |
| 36.3 | 41.9 | 32.9 | 30.9 | 31.8 | 41.1 | 32.3 | 30.3 | 32.2 |
| 33.2 | 44.1 | 34.9 | 32.5 | 34.4 | 43.0 | 34.0 | 32.4 | 34.1 |
| 30.0 | 44.2 | 36.1 | 34.1 | 35.9 | 43.6 | 34.9 | 33.7 | 36.2 |
| 26.8 | 45.1 | 37.3 | 35.4 | 37.5 | 42.9 | 35.9 | 34.3 | 36.7 |
| 23.7 | 45.2 | 37.6 | 36.3 | 38.6 | 42.8 | 35.6 | 34.5 | 36.9 |
| 20.5 | 45.6 | 38.1 | 36.5 | 38.8 | 42.7 | 35.6 | 34.3 | 37.1 |
| 17.4 | 45.2 | 37.8 | 36.3 | 38.5 | 41.7 | 35.0 | 33.5 | 35.9 |
| 14.2 | 43.8 | 36.7 | 35.4 | 37.4 | 40.1 | 33.4 | 31.6 | 34.1 |
| 11.1 | 42.6 | 34.3 | 33.4 | 35.4 | 37.5 | 31.0 | 30.1 | 32.4 |
| 7.9 | 40.0 | 32.2 | 30.5 | 32.8 | 35.4 | 28.6 | 27.0 | 29.3 |
| 4.7 | 38.4 | 29.0 | 27.0 | 30.1 | 34.0 | 25.4 | 23.8 | 26.6 |
| 1.6 [b] | 46.9 | 35.6 | 34.0 | 38.2 | 41.8 | 31.2 | 29.8 | 33.4 |
| **Stripe Average** | **39.9** | **31.6** | **29.8** | **31.7** | **37.6** | **29.8** | **28.2** | **30.3** |

[a] Top of LEU fuel foil in upflow reactor is at 22 ⅜ inch (56.8325 cm).
[b] Bottom of LEU fuel foil in upflow reactor is at zero.

# 4 Thermal – Hydraulic Parameters

## 4.1 Coolant Characteristics

The nominal channel coolant velocities for the LEU MITR core are shown in Table 9. These mass flow rates are calculated based on the full width of the coolant channel including fueled and unfueled, finned and unfinned regions. The end channel values are based upon the nominal conditions, other than the conservative gap size of 50.5 mil (end nozzles touching a structural wall). The values in Table 9 for mass flow rate and velocity are secondary DDE design considerations after meeting power, temperature and burnup characteristics of an MITR LEU core. Considerations such the entrance and exit effects should be considered so that the flow conditions are representative of the geometry of MITR without, for example, localized fluid jets due to orifices or other flow conditioners.

Table 9. Nominal LEU coolant characteristics for MITR.

| | **Interior Channel** | **End Channel** |
|---|---|---|
| Channel Gap (mil from fin-tip) | 72 mil | 50.5 mil |
| Mass Flow Rate (kg/s) | 0.25 | 0.16 |
| Velocity (m/s) | 2.1 | 1.9 |

## 4.2 Fuel Plate Characteristics

RELAP5 modeling was performed in order to determine steady state temperatures in the nominal 7 MW MITR core. At the location of peak temperature in the nominal 7 MW LEU core, the model yields a peak LEU fuel temperature of 102 ºC, and peak surface temperature of the cladding of 92 ºC. DDE irradiation temperatures should target to meet, or modestly exceed, these temperatures. As a part of this experiment design, uncertainties in the irradiation experiment should be considered to determine the appropriateness of the intended irradiation target.

# 5 Conclusions

In order to plan for the conceptual design and test plan of a U-10Mo fueled DDE element prototypic of an MITR LEU element, or a portion of an MIT LEU element, this work has presented parameters relevant to a DDE test reactor irradiation. Whereas the parameters in this work provide a basis for the design of the element, it should be noted that the final element design may change prior to conversion of the MITR reactor to LEU fuel. Presently work is ongoing in order to improve fabricability of the element, and further design iterations may be required depending on fuel performance and fabrication constraints.

Through an ongoing technical collaboration, the Massachusetts Institute of Technology and Argonne National Laboratory have developed the conceptual design parameters in this report. Further cooperative work should continue between these parties, and Idaho National Laboratory where the DDE irradiation is planned. Such cooperation should be included each stage of DDE experiment planning and review. In particular, in order to plan a DDE irradiation appropriate to MITR, planned irradiation target conditions, as well as the uncertainties in achieving these in the DDE experiment require further consideration and agreement between the parties involved.

This set of analyses, performed with the feasibility design, serve as a reference conceptual design for key parameters to be used for the irradiation of the DDE in a test reactor prior to LEU conversion of MITR with elements of the same fuel element geometry and construction as the DDE. The DDE is an experiment performed within the context of an ongoing and larger campaign to qualify U-10Mo fuel for use in various reactors. The purpose of the DDE irradiations is a limited-scale demonstration that an element with geometry and irradiation history different from those previously irradiated will perform adequately. Prior to fully describing the requirements of a final DDE experimental plan, it is first necessary to know the parameters of the predecessor campaign where the heat flux, fuel temperature, and fission density histories are given from beginning to end of experiment along with specific as-built test geometry and material loadings. Also, in order for the results of fuel performance from the fuel qualification campaign to apply to the DDE, both must share the same methods of fabrication in order to support the basis for qualification of the fuel for use in the MITR reactor conversion to LEU fuel.

# References

[1] E.H. Wilson, T.H. Newton, Jr., A. Bergeron, N. Horelik, and J.G. Stevens, "Comparison and Validation of HEU and LEU Modeling Results to HEU Experimental Benchmark Data for the Massachusetts Institute of Technology MITR Reactor," ANL-RERTR-TM-10-41, Argonne National Laboratory, December, 2010.

[2] T.H. Newton, Jr., E.H. Wilson, A. Bergeron, N. Horelik, and J.G. Stevens, "Neutronic Analyses for HEU to LEU Fuel Conversion of the Massachusetts Institute of Technology MITR Reactor," ANL-RERTR-TM-10-40, Argonne National Laboratory December 2010.

[3] L. Hu, K. Chiang, E.H. Wilson, F.E. Dunn, T.H. Newton, Jr., and J.G. Stevens, "Thermal Hydraulic Limits Analysis for LEU Fuel Conversion of the MIT Reactor," MITNRL-12-01, Massachusetts Institute of Technology, March 2012.

[4] E.H. Wilson, N. Horelik, F.E. Dunn, T.H. Newton, Jr., L. Hu, and J.G. Stevens, "Power distributions in Fresh and Depleted LEU and HEU Cores of the MITR Reactor," ANL-RERTR-TM-12-3 Revision 0, Argonne National Laboratory, February, 2012.

[5] Lin-wen Hu, T.H. Newton, E.H. Wilson, J.G. Stevens, "Preliminary Safety Analysis Report Methodologies and Scenarios for LEU Fuel Conversion of the MITR Reactor," MITNRL-11-01, MIT Nuclear Reactor Laboratory, Massachusetts Institute of Technology, Cambridge, Massachusetts, April, 2011.

[6] MITR-II "Fuel Element Assembly," drawing R3F-201-4, MIT Nuclear Reactor Laboratory, Massachusetts Institute of Technology, Cambridge, Massachusetts.

[7] Z. Xu, P. Hejzlar, and M.S. Kazimi, "MCODE, Version 2.2 — An MCNP-ORIGEN Depletion Program," Center for Advanced Nuclear Systems, Massachusetts Institute of Technology, Cambridge, Massachusetts, April 2006.

[8] A.G. Croff, "A User's Manual for the ORIGEN2 Computer Code," ORNL/TM-7175, Oak Ridge National Laboratory (1980).

[9] "MCNP - A General Monte Carlo N-Particle Transport Code, Version 5 User's Guide Manual," X-5 Monte Carlo Team, LA-UR-03-1987, Los Alamos National Laboratory, April, 2003.

[10] A.B. Robinson and M.R. Finlay, "RERTR-7 Post Irradiation Examination (PIE) Letter Report", INL/EXT-07-13271, Idaho National Laboratory, September, 2007.

**Nuclear Engineering Division**
Argonne National Laboratory
9700 South Cass Avenue, Bldg. 208
Argonne, IL 60439-4842

www.anl.gov